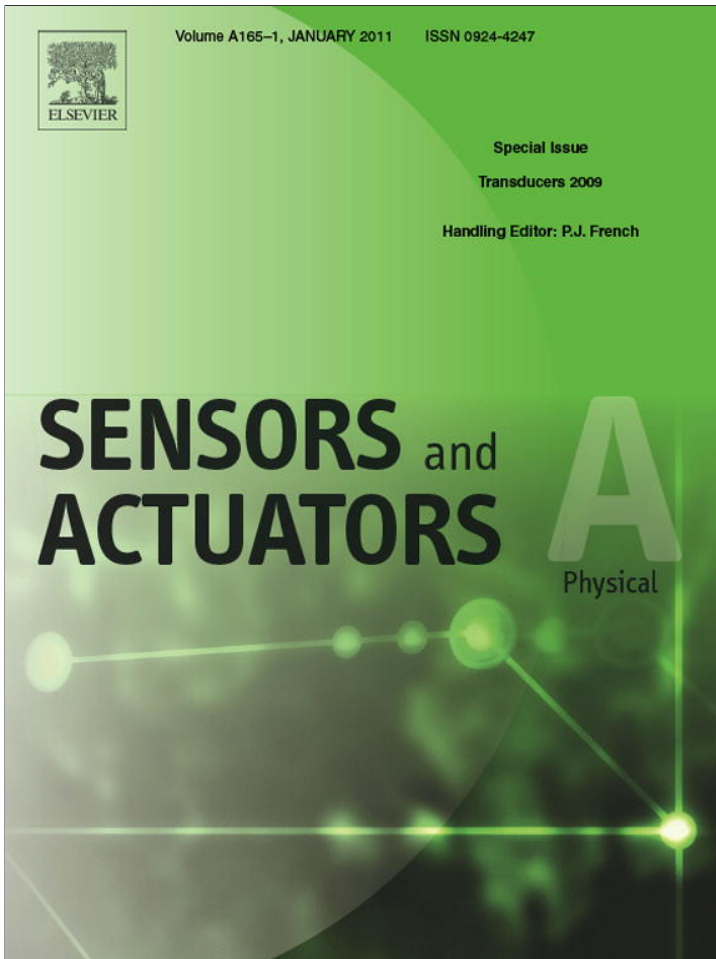


Provided for non-commercial research and education use.
Not for reproduction, distribution or commercial use.

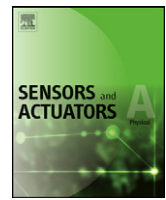


This article appeared in a journal published by Elsevier. The attached copy is furnished to the author for internal non-commercial research and education use, including for instruction at the authors institution and sharing with colleagues.

Other uses, including reproduction and distribution, or selling or licensing copies, or posting to personal, institutional or third party websites are prohibited.

In most cases authors are permitted to post their version of the article (e.g. in Word or Tex form) to their personal website or institutional repository. Authors requiring further information regarding Elsevier's archiving and manuscript policies are encouraged to visit:

<http://www.elsevier.com/copyright>



Analysis of high-*Q* gallium nitride nanowire resonators in response to deposited thin films

J.R. Montague^{a,*}, M. Dalberth^b, J.M. Gray^a, D. Seghete^c, K.A. Bertness^d, S.M. George^c, V.M. Bright^e, C.T. Rogers^a, N.A. Sanford^d

^a University of Colorado, Dept. of Physics, 390 UCB, Boulder, CO 80309, USA

^b Cambridge NanoTech Inc., 68 Rogers St., Cambridge, MA 02142, USA

^c University of Colorado, Dept. of Chemistry and Biochemistry, Boulder, CO 80309, USA

^d Optoelectronics Division, NIST, Mailstop 815.04, 325 Broadway, Boulder, CO 80305-3328, USA

^e University of Colorado, Dept. of Mechanical Engineering, Boulder, CO 80309, USA

ARTICLE INFO

Article history:

Available online 27 March 2010

Keywords:

Atomic layer deposition
Crystal resonators
Gallium compounds
Molecular beam epitaxial growth
Nanoelectronics
Nanowires
Piezoelectric oscillations
Piezoelectric semiconductors
Q factor
Resonators
Wide band gap semiconductors
III-V semiconductors

ABSTRACT

Gallium nitride nanowires (GaN-NWs) are systems of interest for mechanical resonance-based sensors due to their small mass and, in the case of *c*-axis NWs, high mechanical quality (*Q*) factors of 10,000–100,000. We report on singly-clamped NW mechanical cantilevers of roughly 100 nm diameter and 15 μm length that resonate near 1 MHz and describe the behavior of GaN-NW resonant frequencies and *Q* factors following coating with various materials deposited by atomic layer deposition (ALD), including alumina (Al_2O_3), ruthenium (Ru), and platinum (Pt). Changes in the GaN-NW resonant frequencies with ALD deposition clearly distinguish conformal film growth versus island film growth. Conformal films lead to a stiffening of the NW and typically increase resonant frequency, whereas island films simply increase the NW mass and cause decreased resonant frequencies. We find that conformal growth of ALD alumina leads to stiffening of ~4 kHz per nm of alumina, in agreement with previously measured material properties. Conformal growth of Ru and Pt, respectively, qualitatively confirm our analytical predictions of positive and negative resonant frequency shifts. Island growth of ALD Ru has demonstrated a decrease in resonant frequency consistent with mass loading of ~0.2 fg for a 150 ALD-cycle film, also consistent with analytical predictions. Resonant *Q* factors are found to decrease with ALD film growth, offering the additional possibility of studying mechanical dissipation processes associated with the ALD-NW composite structures.

© 2010 Elsevier B.V. All rights reserved.

1. Introduction

Gallium nitride (GaN) nanowires (NWs) are being intensively studied for possible applications in such areas as gas sensing [1], signal processing [2,3], electronic circuitry [4], and light emitting diode (LED) structures [5,6]. In this paper, we investigate the possible use of GaN-NWs in resonant mass sensor applications. NWs are strong candidates for resonant mass sensors, due to the benefits provided by small sensor mass, and high mechanical quality factors [7–11], both of which are provided in the GaN-NW system. Examples of as-grown nanowires are shown in Fig. 1. Briefly, the GaN-NWs investigated here are grown, catalyst free, via gas source molecular beam epitaxy on Si (1 1 1) substrates [12]. The NWs have a defect-free, wurtzite crystal structure with their *c*-axis along the long axis of the NW, have diameters approximately 200 nm, and

overall lengths from 15 μm to 20 μm. The average total NW mass is roughly 2 pg and their lowest, singly-clamped, mechanical resonance frequencies are near 1 MHz. The quality (*Q*) factor (defined as the ratio of the resonant frequency to the resonance full width at half maximum power, or FWHM) is in the range 10^4 to 10^5 and has been measured as high as 10^6 [13]. In this paper, we describe the use of GaN-NWs to study ALD film deposition through the shifts in nanowire resonant frequency and *Q* factors. Our results show that NW vibrational frequencies can readily distinguish conformal film growth from island growth, and mode *Q* factors are sensitive to mechanical dissipation losses in the ALD films. Thus, GaN-NW mechanical resonators have great potential for monitoring ALD film growth mechanisms.

2. Resonance theory and measurements

A simple picture of how NW mechanical resonators are sensitive to thin film properties is provided by beam theory for the cantilever flexural resonant modes of a singly-clamped beam [14]. Eq. (1) gives

* Corresponding author. Tel.: +1 303 492 7940; fax: +1 303 492 3352.

E-mail address: Joshua.Montague@Colorado.edu (J.R. Montague).

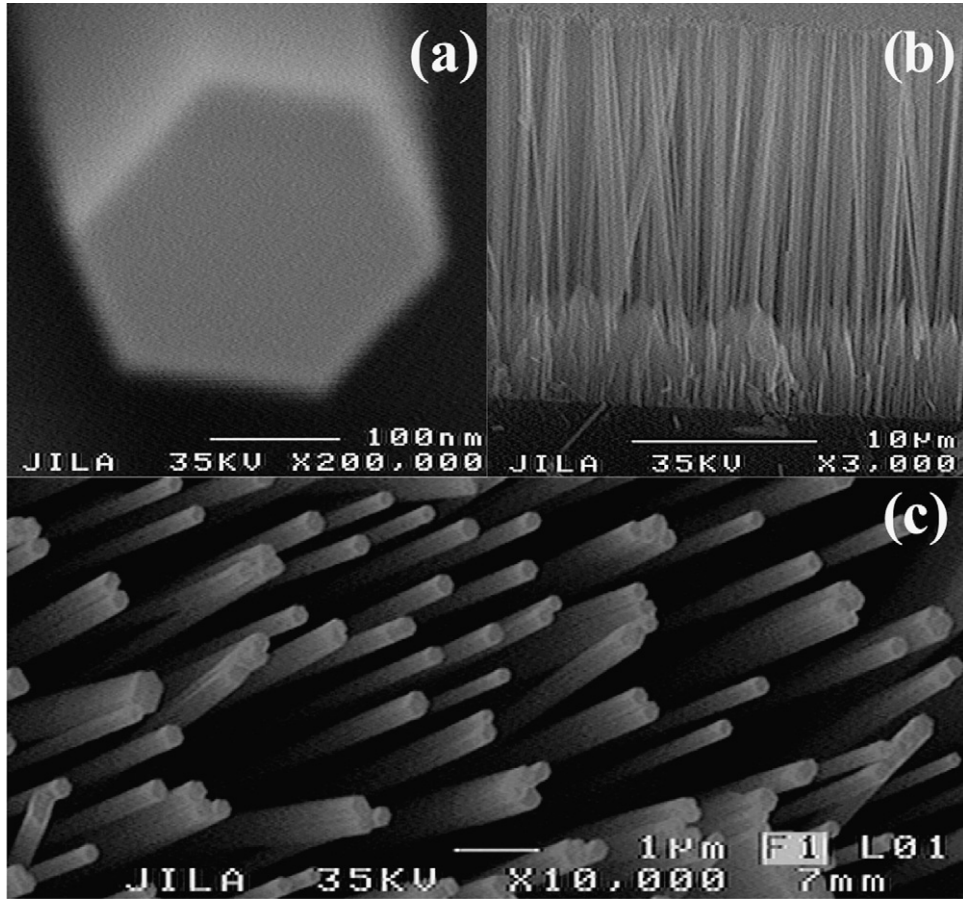


Fig. 1. Electron micrographs of as-grown GaN-NWs [12]. (a) Typical hexagonal cross-section of *c*-axis, wurtzite crystal structure. (b) Side view of nanowire growth from GaN matrix layer to 15–20 μm . (c) Angled plan view of as-grown nanowires.

the resonant frequency for the *n*th mode of such a beam:

$$f_0 = \frac{1}{2\pi} \sqrt{\frac{\kappa}{\mu}} \frac{\alpha_n^2}{L^2}. \quad (1)$$

Here, κ and μ are, respectively an effective stiffness and effective mass per unit length, α_n is a dimensionless number determined by the boundary conditions, and L is the beam length. For the lowest-order, fundamental frequency of a singly-clamped beam, $\alpha_0 = 1.875$. For simple geometries, $\kappa = EI_2$, where E is the Young's modulus, I_2 is the second moment of the beam (e.g. $\pi r^4/4$ for a circular cross-section with radius r , $5\sqrt{3}a^4/16$ for a hexagonal cross-section with side length a) and $\mu = \rho A$, where ρ is the density and A is the beam's cross-sectional area. Depositing a film on such a beam can change the resonant frequency by two competing effects. First, the added mass of the film increases the total mass per unit length, and thereby can cause a decrease in resonant frequency. Second, the combination of film Young's modulus and degree of continuity can increase the stiffness of the beam and lead to an associated increase in resonant frequency. We find that both of these effects may occur with different ALD coating materials.

As an illustrative example, useful for comparison to our data, consider a cylindrical beam of material 1 (density ρ_1 , Young's modulus E_1) and initial radius, r , with an additional uniform thickness, t , of material 2 (ρ_2, E_2). The lowest-order resonant frequency is found within Euler–Bernoulli beam theory to be

$$f_0 = \frac{1}{4\pi} \left[\frac{E_1 r^4 + E_2 ((r+t)^4 - r^4)}{\rho_1 r^2 + \rho_2 ((r+t)^2 - r^2)} \right]^{1/2} \left(\frac{1.875}{L} \right)^2. \quad (2)$$

Fig. 2 shows the predicted resonant frequency versus ALD film thickness starting with an initial resonant mode at 1 MHz, for the three ALD materials studied in this work: Al_2O_3 (alumina), ruthenium (Ru), and platinum (Pt). The calculated resonant frequencies using a cylindrical cross-section overestimate those of the hexagonal cross-section by approximately 9%.

In the limit $t \ll r$ appropriate for thin layers, we find a first-order shift in the resonant frequency, δf , from the $t=0$

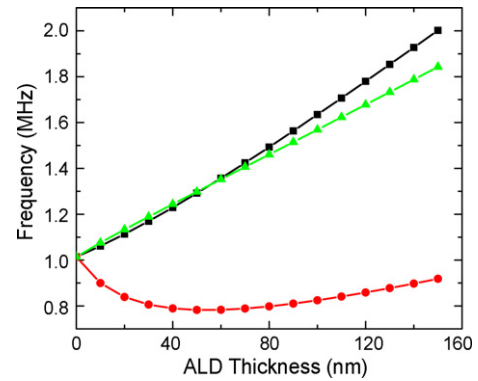


Fig. 2. Predicted resonant frequency shifts for the three ALD materials studied in this work, assuming conformal growth. Squares, triangles, and circles correspond, respectively, to alumina, Ru and Pt. The initial, bare GaN-NW resonance is set to 1 MHz. The ALD material properties used are described in the text. With alumina and Ru, stiffening of the nanowire dominates the mass loading, causing an overall increase in resonant frequency. For high-density Pt, mass loading dominates initially, followed by stiffening for thicker films. Our experimental results qualitatively confirm these trends.

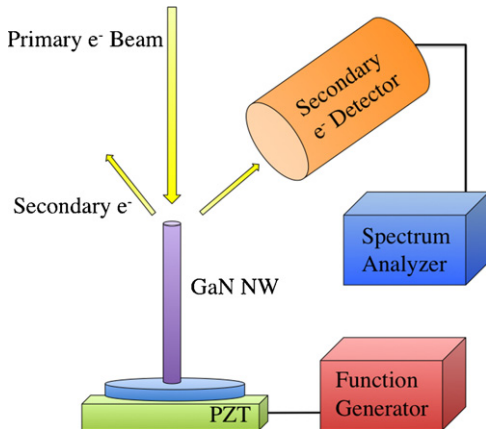


Fig. 3. Schematic of experimental setup for obtaining resonance measurements of coated and uncoated nanowires within an electron microscope chamber.

value

$$\delta f = f_0 \cdot (2\tilde{E} - \tilde{\rho}) \cdot \frac{t}{r}, \quad (3)$$

where f_0 is the original resonant frequency and \tilde{E} and $\tilde{\rho}$ are, respectively, the ratios of the film's (material 2) Young's modulus to GaN's Young's modulus, and film density to GaN density. We note that for long, thin beams such as GaN-NWs, the ratio f_0/r is independent of radius, indicating that δf should be similar even for nanowires of rather different initial f_0 and r . This result is confirmed in Section 2.1.

Resonant properties of the GaN-NWs were measured in vacuum (below 10^{-4} Pa) in a scanning electron microscope (SEM), as illustrated schematically in Fig. 3. Portions of the Si substrate containing the nanowire matrix and as-grown nanowires were mounted atop a lead zirconate titanate (PZT) shear mode, piezoelectric actuator. The electron beam was placed in spot mode and positioned on the edge of a nanowire. In one mode of detection a broadband white noise signal is applied to the piezoelectric stack by a function generator (FG), and the output of the secondary electron detector is fed to a real-time spectrum analyzer. Operation in the electron microscope environment offers the crucial advantages of allowing measurement of the resonant properties of ensembles of many nanowires and the ability to locate and remeasure the entire ensemble after additional processing steps.

A typical resonant power spectrum resulting from the application of white noise is shown in Fig. 4a. The general relationship between a driving signal and the frequency response or power

spectrum is given by

$$P(\omega) = F(\omega) \cdot |H(\omega)|^2. \quad (4)$$

Here, $F(\omega)$ is the Fourier transform of the driving force, and $H(\omega)$ is the harmonic transfer function, given by

$$H(\omega) = \frac{A}{\omega^2 - \omega_0^2 - i\omega\Gamma}, \quad (5)$$

where Γ is the damping factor, ω_0 is the angular resonant frequency, and A is an amplitude. If the driving function is assumed to be white noise, then $F(\omega)$ is a constant and the power spectrum is proportional to $|H(\omega)|^2$. As shown in Fig. 4, the resulting resonance lines can be fitted with a standard Lorentzian curve – appropriate for a damped harmonic oscillator – and sidebands resulting from mixing products between NW motion and 60 Hz noise in SEM circuitry. The Q factor is then determined by finding the ratio of the resonant frequency to the FWHM of the Lorentzian curve, $\omega_0/\Delta\omega_{FWHM}$.

In a second mode of detection, the FG applies a sinusoidal signal and the frequency of excitation is swept through the nanowire resonance. This mode of measurement provides visual confirmation of nanowire resonance via standard secondary electron imaging, as shown in Fig. 5. In this mode, the spectrum analyzer can also be replaced with a radio frequency (RF) lock-in detector, allowing the extraction of a complex Lorentzian lineshape.

Based on Eq. (1), a beam with a perfectly hexagonal cross-section will have two orthogonal degenerate resonant frequencies with the fundamental mode shape. As shown in Fig. 5, slight growth irregularities leading to uneven nanowire side lengths (while still maintaining internal angles of 120°) produce two orthogonal, non-degenerate resonant frequencies with the fundamental mode shape. We have also used a three-dimensional finite element model (FEM) of the NWs based on a quadratic 10 node brick element to confirm this mode splitting.

The GaN-NWs studied in this work tended to all be approximately the same length. Thus, differences in the resonant frequencies of individual NWs result from differing cross-sectional area. The GaN-NWs measured typically had radius in the range 50–200 nm.

2.1. Conformal ALD alumina films

ALD alumina films were deposited on NW samples at 120°C , with $\text{Al}(\text{CH}_3)_3$ and H_2O as precursors. The growth rate was about 1.2 \AA per cycle. Fig. 4(a) and (b), respectively, shows an example of a typical resonance for a bare, as-grown GaN-NW, and the same nanowire with a thin coating of ALD alumina. As we have reported

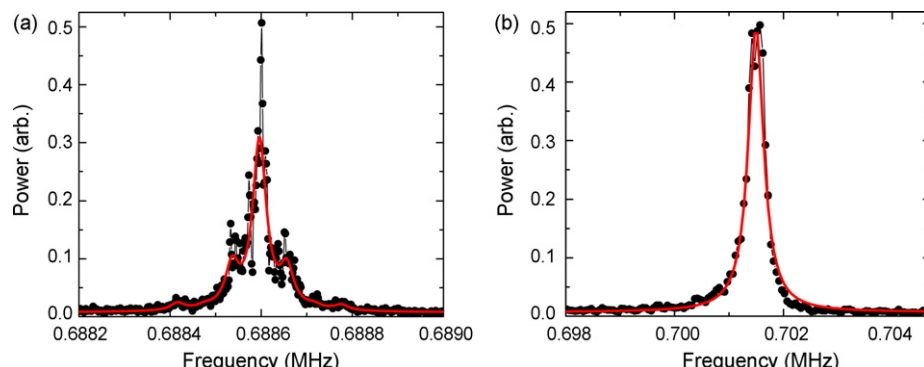


Fig. 4. Fundamental resonant peak for a single GaN-NW. (a) Spectrum of bare GaN-NW, before ALD coating. Solid curve indicates a Lorentzian fit showing resonant frequency of $f_0 = 688,596 \pm 1$ Hz, $Q = 19,000 \pm 2000$, and sidebands resulting from mixing products between NW motion and 60 Hz noise in secondary electron detection circuitry. (b) Spectrum of the same nanowire after 4.6 nm ALD alumina coating. Solid curve indicates a Lorentzian fit showing resonant frequency of $f_0 = 701,495 \pm 9$ Hz, $Q = 2000 \pm 200$. Note enlarged frequency scale and the increase in linewidth that obscures 60 Hz sidebands.

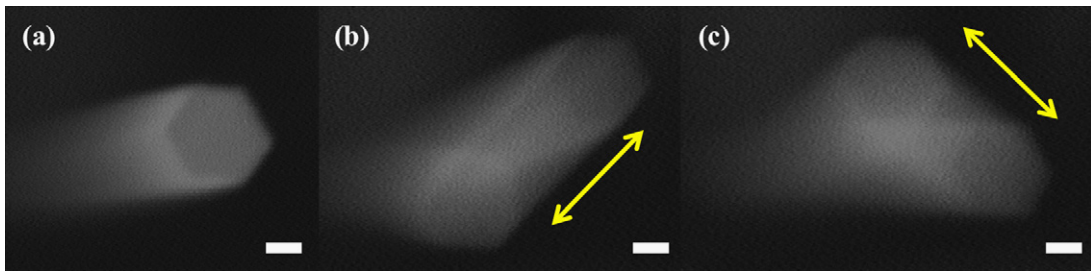


Fig. 5. Example of lowest-order, non-degenerate resonant modes of the single GaN-NW shown in (a), resulting from small geometric irregularity. In (b) and (c), respectively, the NW is driven at its fundamental frequencies near 851 kHz and 691 kHz. Periodic motion results in apparent “fanning” of NW when viewed in an SEM. Accompanying arrows illustrate the direction of NW motion. All scale bars are 100 nm.

previously [13], these *c*-axis GaN-NWs show Q factors $> 10^4$ near 1 MHz. The as-grown GaN-NW resonances are narrow enough to show well isolated 60 Hz sidebands (and harmonics) that arise from the electron microscope environment. When the nanowires have been coated with a conformal layer of ALD alumina, we observe both an increase in the resonant frequency and a broadening of the resonance lineshape in the power spectra (note the expanded frequency scale in Fig. 4b).

Fig. 6 shows the progression of resonant line shift for a single mode of one GaN-NW with an initial resonance near 695 kHz. The figure shows three sequential shifts upward in resonant frequencies due to three ALD alumina growths of, respectively 4.6 nm, 4.5 nm and 3.9 nm, associated broadening of the resonance, and a return to lower frequency and narrow line upon removal of the ALD film by aqueous hydrofluoric acid (HF) etching and an oxygen (O_2) plasma reactive ion etch (RIE). The robust nature of the GaN-NWs to repeated film growth and etching procedures shows that they have promise as sensors for multi-step processing.

In Fig. 7, the resonant frequencies of as-grown GaN-NWs are presented for an ensemble of six nanowires following the same consecutive 4.6 nm, 4.5 nm, and 3.9 nm ALD alumina depositions shown in Fig. 6. Again, after HF and O_2 plasma RIE, GaN-NW resonant frequencies were restored very nearly to their original values. Most nanowires show a nearly constant relation between increase in resonant frequency and thickness of deposited ALD alumina, as is expected from the simple beam theory of Section 2.

Occasionally, we find abrupt increases in nanowire resonant frequencies. An example of this behavior is shown in Fig. 7. The resonance, which began near 530 kHz, follows the resonance shift

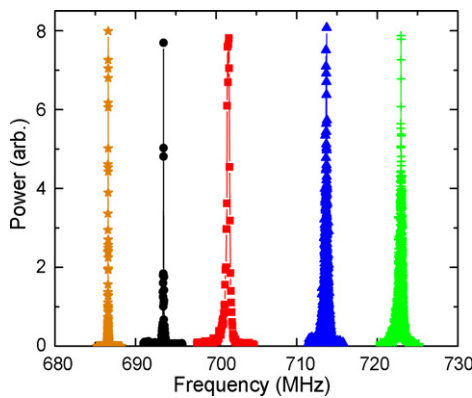


Fig. 6. Change in resonant frequency for one mode of a single GaN-NW after ALD alumina depositions and removal. The bare nanowire (circles) is sequentially coated with ALD thickness of 4.6 nm (squares), 4.5 nm (triangles), and 3.9 nm (crosses). After aqueous HF etching to remove the ALD alumina, followed by a brief O_2 RIE exposure to remove organics, the resonant frequency drops to near original value (stars). Note also the increased linewidth in ALD spectra, as compared with bare/etched spectra.

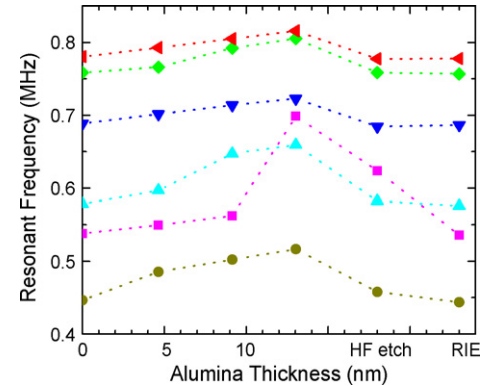


Fig. 7. Increase in GaN-NW resonant frequency after ALD alumina coatings of 4.6 nm, 4.5 nm, and 3.9 nm. “HF etch” and “RIE” correspond, respectively, to a hydrofluoric acid etch and O_2 plasma RIE that remove the ALD film and return the nanowires to their original resonance positions. In order of increasing original resonant frequencies, the data correspond to nanowires with side lengths of 128 nm (circles), 115 nm (squares), 150 nm (up-pointing triangles), 154 nm (down-pointing triangles), 137 nm (diamonds), and 128 nm (left-pointing triangles). The abrupt increase in the resonant frequency near 13 nm of ALD of the nanowire starting at ~530 kHz is attributed to shortening of the nanowire by filling of the matrix layer, as described in Section 2.1.

common to the other five nanowires until the third alumina deposition. After this deposition, the resonance position is observed to increase by ~ 125 kHz. Such large increases are observed to occur only once for any one nanowire and simultaneously affect both orthogonal modes. We have attributed this behavior to the effective shortening of the nanowire due to ALD film filling the matrix layer at the nanowire base, as illustrated schematically in Fig. 8. The resulting clamping of the nanowire at a higher position reduces the

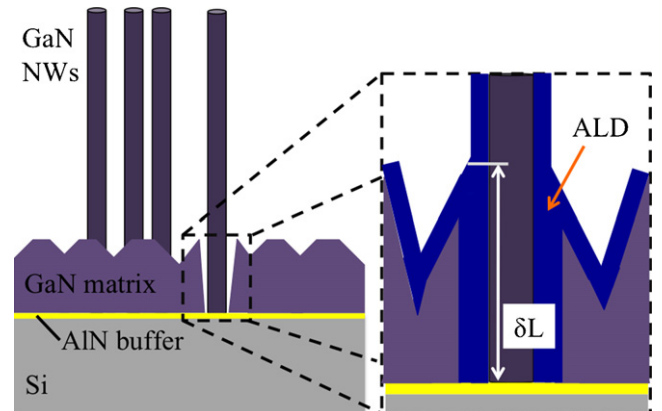


Fig. 8. Schematic of GaN matrix layer filling. When the conformal film on the NW and surrounding GaN matrix material come into contact, the NW is effectively shortened by a length δL , increasing its resonant frequency.

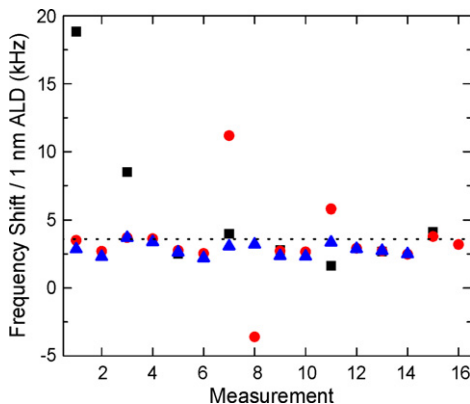


Fig. 9. Distribution of resonant frequency shifts, δf , per nm of deposited ALD for all alumina-coated GaN-NWs studied in this work. Each pair of “Measurements” (i.e. points at $x=1$ and $x=2$, {3, 4}, {5, 6}, etc.) corresponds to the two modes of a single nanowire. Squares, circles, and triangles correspond, respectively, to frequency shifts resulting from the addition of 4.6 nm, 4.5 nm, and 3.9 nm alumina. The average shift of 3.6 kHz/nm ALD alumina is shown by the dotted line.

beam length and increases the resonant frequency, as shown in Eq. (1).

Data from both modes of each GaN-NW are presented over the course of consecutive ALD alumina depositions in Fig. 9. In good agreement with the first-order calculation of Eq. (3), a consistent, positive shift of $\delta f \approx 3.6$ kHz per nm ALD alumina is shown. If we use the uncertainty in resonant position from the ALD-coated nanowire given in Fig. 4b of 9 Hz, we find that the GaN-NW resonators should be able to resolve sub-monolayer coverage, making them useful for studying early stages of ALD growth.

The material properties of the ALD alumina have been measured previously by Tripp et al. [15]. In that work, the Young's modulus of ALD alumina was calculated in the range $E = 168\text{--}182$ GPa, and density $\rho = 3.03$ g/cm³. As is common with ALD materials, these values are less than their respective bulk values of $E = 370$ GPa and $\rho = 3.97$ g/cm³. Using the material properties given in [15] and the GaN-NW material properties ($E = 300$ GPa, $\rho = 6.2$ g/cm³), Eq. (3) predicts a shift in resonant frequency of 4–5 kHz per nm of added ALD alumina, in good agreement with our measured data.

As-grown GaN-NW FWHM linewidths are typically in the range of 10–100 Hz. As shown in Fig. 10, the addition of an initial 4.6 nm of ALD alumina results in a decrease in Q from an original range of approximately 11,000–40,000 to a coated Q spanning approximately 1000–4000. The deposition of an additional 4.5 nm and

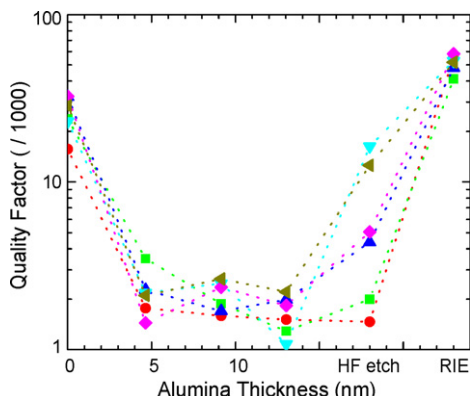


Fig. 10. Decrease of GaN-NW resonator quality (Q) factor after ALD alumina coatings of 4.6 nm, 4.5 nm, and 3.9 nm, followed by restoration via etching. Symbols correspond to the same NWs as in Fig. 7. “HF etch” and “RIE” correspond, respectively, to a hydrofluoric acid etch and O₂ plasma RIE. Note after O₂ plasma RIE, all Q factors have been improved relative to initial values.

3.9 nm of ALD alumina produces similar additional increases in resonant frequencies, but has very little additional effect on the composite resonator's Q factor. After wet etching in HF and putting the sample in an O₂ plasma RIE, GaN-NW Q factor is restored to or is greater-than the initial, as-grown range, spanning 40,000–60,000. Since GaN-NWs are known to have virtually no native oxide growth [16], this increase in Q may indicate a modest accumulation of organic contaminants on the nanowire after growth, but prior to use for ALD sensing.

2.2. Conformal ALD metallic films

A study of ALD films of the transition metals Pt and Ru provided a qualitative confirmation of the behavior predicted by Eq. (2), and established by our alumina studies. Details of the results are listed in Table 1. Single growth thickness of 40 nm (Pt) and 12.7 nm (Ru) were selected to assure continuous films.

Pt films were deposited at 270 °C, with a (Me₃PtCpMe) or (CH₃)₃(CH₃C₅H₄)Pt precursor and with O₂ as a reactant. The growth rate was 0.33 Å per cycle. For this Pt film, the average measured resonance shift was $\delta f \approx -28$ kHz. Most of the measured nanowires (10 of 16) had a reduced resonant frequency consistent with addition of a high-density material, as predicted by both Eq. (3) and Fig. 2. The remaining six showed the increase in resonance position described in Section 2.1. Disregarding the nanowires that show matrix filling, the average shift was $\delta f \approx -110$ kHz. The addition of a conformal Pt film also typically led to a broadening of the resonant peak. Most measured nanowires demonstrated a decrease in their Q factor. The initial Q range of about 2000 to 2,000,000 (mostly in the range 10⁴ to 10⁵) was reduced to a post-ALD Pt range of about 2000–10,000.

Ru films were deposited at 270 °C, with a (C₅H₅)₂Ru precursor and O₂ as a reactant. After nucleation, the growth rate was 0.45 Å per cycle. For this Ru film, the average measured resonance shift was $\delta f \approx 289$ kHz. Again, this shift (11 of 16 nanowires) toward higher resonant frequency is qualitatively consistent with the behavior shown in Fig. 2. As was the case with both conformal films of alumina and Pt, the conformal coating of Ru also led to resonance broadening. For all nanowires measured, Q decreased from its initial value. Here, the original range of about 11,000–80,000 decreased to a post-ALD Ru range of about 1000–4000.

More rigorous comparison of the predictions of Eq. (2) and our measured data will be useful after thorough investigation of the ALD film properties. As described in Section 2.1, the ubiquitous use of ALD alumina in the field of microelectromechanical systems (MEMS) has led to thorough characterization of its properties. Similar investigation of the Pt and Ru films used in this work can be compared to known bulk properties (Pt: $E = 168$ GPa, $\rho = 21,450$ kg/m³; Ru: $E = 447$ GPa, $\rho = 12,450$ kg/m³).

After both Pt and Ru film depositions, a small number of measured GaN-NWs demonstrated an increase in resonant frequency whose magnitude greatly exceeded the prediction of Eq. (2). This behavior has also been attributed to the filling of the matrix layer, as described in Section 2.1. Cross-sectional sample analysis via focused ion beam (FIB) or tunneling electron microscope (TEM) may provide insight into the matrix filling effect to which the discrepancy has been attributed.

2.3. Discontinuous ALD Ru films

During the early growth stages of some ALD materials, nucleation occurs in isolated “islands.” Before these islands coalesce, the discontinuous film will increase the effective resonator mass (in Eq. (1)) without necessarily contributing significantly to the resonator's effective stiffness. By measuring a shift in the resonant frequency, Eq. (1) also lets us calculate the amount of material that was deposited on the resonator.

Table 1
Results from ALD coatings of Pt and Ru on GaN-NWs.

ALD material	ALD thickness (nm)	Number of nanowires [modes]	Average resonant frequency shift (kHz)
Pt	40	10 [20]	-108 ± 44
Ru	12.7 ^a	11 [19]	$+289 \pm 142$
Ru	2 ^b	12 [24]	-19 ± 5

^a Greater precision results from XRR measurements of film.

^b The 150-cycle growth of Ru was not a continuous film, as described in Section 2.3. AFM measurements of a similar film showed islands of vertical height less than or equal to 2 nm.

The ALD Ru presented in Section 2.2 was also studied as a discontinuous film on GaN-NWs. We measured nanowire resonant frequencies and Q factors after just 150 ALD cycles. This deposition period was chosen because it was believed to occur between the nucleation of deposition species and island coalescence. Most of the nanowires studied (13 of 16) demonstrated a decrease in frequency, with the average decrease being $\delta f \approx -7$ kHz. Disregarding the data points indicating an increase in resonant frequency (possibly attributed to the matrix filling mechanism mentioned in Section 2.1), the average resonance shift is $\delta f \approx -19$ kHz. This result is included in Table 1. Using the Ru material data presented in Section 2.1, Eq. (5) gives good agreement, also predicting a resonant frequency shift of $\delta f \approx -16$ kHz.

By expanding Eq. (1), the measured shift in resonance position δf due to the addition of a mass $\delta m \ll m$ can be used to calculate the value of the added mass δm . After measuring the nanowire dimensions in the SEM, using the measured δf , and using XRR data on the Ru film, we calculate an average of $\delta m = 0.2$ fg of material added to the nanowires by the discontinuous ALD Ru.

An atomic force microscope (AFM) was also used to analyze substrates with 150 cycles of the same Ru film (not shown). Using the areal island density and height measured in that analysis, together with the XRR material data, we calculated the mass that should have been deposited to be on the order of 0.1 fg, in good agreement with δm calculated from frequency shifts.

During the resonance measurements on discontinuous Ru, typical resonant frequency uncertainties were on the order of 10 Hz. Considering the measured 16 kHz shift in resonance position for 0.2 fg, we calculate an approximate mass resolution on the order of 0.2 ag with a 1 s averaging time. This resolution is high enough to detect single cycles of the ALD process.

Though the surface coverage of the 150-cycle ALD Ru material should be far less than that of the continuous films, there was still a significant decrease in the nanowire Q. The initial, bare GaN-NW range of about 2000–3,000,000 is reduced to a range of about 400–50,000.

3. Conclusion

GaN-NWs with large intrinsic Q factor (10^4 to 10^6) have been investigated for their potential use in high-resolution thin film deposition applications. Deposition of discontinuous ALD thin films cause NW mechanical resonance frequencies to decrease due to simple mass loading. The NW resonant frequencies allowed us to sense mass loading at the sub-femtogram level, with sub-attogram resolution with 1 s averaging. In comparison, continuous ALD thin films can cause mechanical resonant frequencies to increase, allowing a clear indication of conformal ALD growth. Simple analytical models of the resonant frequencies are in good qualitative agreement with our observations. All conformal coatings resulted in frequency shifts on the order of a few kilohertz per nanometer, frequency shifts that are easily detectable due to the high intrinsic Q factor of the GaN-NWs. Finally, the notable decrease in GaN-NW resonance Q factors with even nanometer thicknesses of ALD material indicate that Q may be used as a probe for early stages of ALD growth.

Acknowledgements

The studies conducted by the corresponding author from the University of Colorado - Boulder are supported by the DARPA Center on Nanoscale Science and Technology for Integrated Micro/Nano-Electromechanical Transducers (iMINT) funded by DARPAN/MEMS S-T Fundamentals Program (HR0011-06-1-0048) (Dr. D.L. Polla, Program Manager), and support from the NSF Division of Civil, Mechanical and Manufacturing Innovation under grant #0856261. We thank B.D. Davidson, A.S. Cavanagh, and D. Alchenberger, all at the University of Colorado, for their advice and support.

References

- [1] J.S. Wright, W. Lim, B.P. Gila, S.J. Pearton, J.L. Johnson, A. Ural, F. Ren, Hydrogen sensing with Pt-functionalized GaN nanowires, *Sens. Actuators B* 140 (2009) 196–199.
- [2] J.A. Judge, B.H. Houston, D.M. Photiadis, P.C. Herdic, Effects of disorder in one- and two-dimensional micromechanical resonator arrays for filtering, *J. Sound Vib.* 290 (2006) 1119.
- [3] C.T.C. Nguyen, Frequency-selective MEMS for miniaturized low-power communication devices, *IEEE Trans. Theory Technol.* 47 (1999) 1486.
- [4] A. Motayed, A.V. Davydov, M.D. Vaudin, I. Levin, J. Melngailis, S.N. Mohammad, Fabrication of GaN-based nanoscale device structures utilizing focused ion beam induced Pt deposition, *J. Appl. Phys.* 100 (2006) 114310.
- [5] H.M. Kim, Y.H. Cho, H. Lee, S.I. Kim, S.R. Ryu, D.Y. Kim, T.W. Kang, K.S. Chung, High-brightness light emitting diodes using dislocation-free indium gallium nitride/gallium nitride multiquantum-well nanorod arrays, *Nano Lett.* 6 (2004) 1059–1062.
- [6] A. Kikuchi, M. Tada, K. Miwa, K. Kishino, Growth and characterization of InGaN/GaN nanocolumn LED, *Proc. SPIE* 6129 (2006) 612905.
- [7] K.L. Ekinci, X.M.H. Huang, M.L. Roukes, Ultrasensitive nanoelectromechanical mass detection, *Appl. Phys. Lett.* 84 (2004) 4469.
- [8] B. Ilic, H.G. Craighead, S. Krylov, W. Senaratne, C. Ober, P. Neuzil, Attogram detection using nanoelectromechanical oscillators, *J. Appl. Phys.* 95 (2004) 3694.
- [9] Y.T. Yang, C. Callegari, X.L. Feng, K.L. Ekinci, M.L. Roukes, Zeptogram-scale nanomechanical mass sensing, *Nano Lett.* 6 (2006) 583.
- [10] A.N. Cleland, M.L. Roukes, A nanometre-scale mechanical electrometer, *Nature (Lond.)* 392 (1998) 160.
- [11] T. Thundat, S.L. Sharp, W.G. Fisher, R.J. Warmack, E.A. Wachter, Detection of mercury vapor using resonating microcantilevers, *Appl. Phys. Lett.* 66 (1995) 1563.
- [12] K.A. Bertness, A. Roshko, L.M. Mansfield, T.E. Harvey, N.A. Sanford, Mechanism for spontaneous growth of GaN nanowires with molecular beam epitaxy, *J. Cryst. Growth* 310 (2008) 3154–3158.
- [13] S.M. Tanner, J.M. Gray, C.T. Rogers, K.A. Bertness, N.A. Sanford, High-Q GaN nanowire resonators and oscillators, *Appl. Phys. Lett.* 91 (2007) 203117.
- [14] A. Cleland, Foundations of Nanomechanics, Springer-Verlag, Berlin, Heidelberg, 2003.
- [15] M.K. Tripp, C. Stampfer, D.C. Miller, T. Helbling, C.F. Herrmann, C. Hierold, K. Gall, S.M. George, V.M. Bright, The mechanical properties of atomic layer deposited alumina for use in micro- and nano-electromechanical systems, *Sens. Actuators A* 130–131 (2006) 419–429.
- [16] J.P. Zhang, Y. Wu, G.S. Cheng, M. Moskovits, J.S. Speck, Dislocation-free GaN nanowires, *Microsc. Microanal.* 9 (2003) 342.

Biographies

Joshua R. Montague received his bachelor of arts in physics and mathematical science from Colby College in 2006. He is currently working toward his Ph.D. in physics at the University of Colorado at Boulder studying gallium nitride nanowire (GaN-NW)-atomic layer deposition (ALD) systems.

Mark Dalberth earned his Ph.D. in physics at the University of Colorado-Boulder in 1999 studying the microwave dielectric properties of strontium titanate thin films. He has tapped into various aspects of this thesis work in his succeeding jobs: film

deposition and device fabrication as a process engineer at Phiar Incorporated and MBE growth engineer at Cielo Communications, cryogenic measurement as a post-doc at the National Institute of Standards and Technology, and optics as an optical engineer at Ball Aerospace. He has been at Cambridge Nanotech since July 2008. He enjoys working on new problems and learning new technologies.

Jason M. Gray received his bachelor of arts in physics with a minor in mathematics from the University of Colorado at Boulder in 2004. He is currently a Ph.D. student in physics at the University of Colorado working on gallium nitride nanowire resonator devices.

Dragos Seghete received his B.S. degree with honors in chemistry and mathematics from University of Arkansas, Fayetteville, AR in 2005. He is currently a physical chemistry Ph.D. student at the University of Colorado at Boulder. His research interests include the exploration of new chemistries for the atomic and molecular layer deposition of low density materials and the development of new applications for existing ALD and MLD systems.

Kris A. Bertness is a Project Leader in the Optoelectronics Division of the National Institute of Standards and Technology in Boulder, CO. Her technical focus has been on III-V semiconductor crystal growth, characterization, and device design, including research on nanowires and quantum dots. Prior to joining NIST in 1995, she developed record-efficiency solar cells with a team at the National Renewable Energy Laboratory. She received her Ph.D. in physics from Stanford University.

Steven M. George is a professor of chemistry and chemical engineering at the University of Colorado. Dr. George received his B.S. in chemistry from Yale University (1977) and his Ph.D. in chemistry from the University of California/Berkeley (1983). His research interests are in surface chemistry, thin film growth and nanostructure engineering. He is currently directing an internationally recognized effort focusing on atomic layer deposition (ALD) and molecular layer deposition (MLD). He has

more than 250 publications in a variety of areas. He is a Fellow of American Physical Society (1997) and a Fellow of the American Vacuum Society (2000).

Victor M. Bright is the Alvah and Harriet Hovlid professor of mechanical engineering and the Faculty Director for Discovery Learning, College of Engineering and Applied Science, University of Colorado at Boulder. He is currently the Chair of Mechanical Engineering Department. Prof. Bright's research interests are in micro- and nano-electromechanical systems (MEMS and NEMS). Prof. Bright is a Senior Member of IEEE, a Fellow of ASME, and an author of over 250 journal papers, conference proceedings, and book chapters. He is a Section Editor for the Micromechanics Section of the Journal Sensors and Actuators A: Physical.

Charles T. Rogers is a professor of physics at the University of Colorado. Before joining the faculty in 1992 he was a Member of Technical Staff in Solid State Physics at Bellcore. Prof. Rogers received his Ph.D. degree in applied physics from Cornell University in 1987. His research interests include small devices fabricated with electron-beam lithography, phase transitions and dynamical processes in reduced dimensional systems, and the physics of fluctuations and noise in electronic devices. He is currently Director of the Engineering Physics Program at the University of Colorado. He has published over 100 peer-reviewed papers and has two patents.

Norman A. Sanford is the Project Leader of the Optoelectronic Materials Metrology effort at the National Institute of Standards and Technology, Boulder, CO. He received the Ph.D. in physics from Rensselaer Polytechnic Institute in 1983 for studies of nonlinear magneto-optics. Sanford was awarded the H.B. Huntington prize from Rensselaer, the NIST Bronze Medal, and is a Fellow of the Optical Society of America, and served as an Associate Editor of the Journal of Quantum Electronics. He has authored or co-authored roughly 100 publications, 2 invited book chapters, and holds 14 U.S. patents.